SYNTHESIS AND CATALYTIC EVALUATION OF FERRIERITE-RELATED MATERIALS SYNTHESIZED IN THE PRESENCE OF CO-STRUCTURE DIRECTING AGENTS

Raquel García[1], Ana Belén Pinar[2], Carlos Márquez-Alvarez[3], Enrique Sastre[4] and Joaquín Pérez-Pariente[5,*]

Instituto de Catálisis y Petroleoquímica, CSIC, C/Marie Curie 2, Cantoblanco, 28049 Madrid, Spain; e-mail: [1] rgs@icp.csic.es, [2] abpinar@icp.csic.es, [3] cmarquez@icp.csic.es, [4] esastre@icp.csic.es, [5] jperez@icp.csic.es

Received May 16, 2008
Accepted August 18, 2008
Published online October 3, 2008

We report on the systematic exploration of zeolite synthesis using a combination of organic molecules of different size. The effect of changing the co-structure directing agent, co-SDA, (tetramethylammonium or quinuclidine) and its replacement by sodium cations, when used together with the bulky organic cation 1-benzyl-1-methylpyrrolidinium (bmp) is analyzed and compared with preparations where bmp is replaced by the related cation (*S*)-1-benzyl-2-hydroxymethyl-1-methylpyrrolidinium (bmprol). The tendency to direct the synthesis to ferrierite or ferrierite-like materials depending on the particular combination of bulky organic cation and co-SDA is discussed. The catalytic activity of some of the materials synthesized was tested in the isomerization of *m*-xylene.

Keywords: Ferrierite; Ferrierite layered materials; Template mixture; Fluoride media; Isomerization of *m*-xylene.

Zeolites are a class of aluminosilicates with three-dimensional framework structures built up from corner-sharing SiO_4 and AlO_4 tetrahedra. The main feature of a zeolitic framework is that it contains channels and/or cavities of molecular dimensions, highly uniform in size and shape, which can act as a molecular sieve[1]. Among the applications of zeolitic materials, their use as heterogeneous catalysts is one of the most thoroughly investigated. Indeed, they have been used as catalysts in petrochemical processes for 40 years, mainly in the field of oil refining and basic petrochemistry[2].

Synthesis of zeolitic materials typically involves the use of an organic molecule around which the inorganic framework crystallizes. These compounds are usually referred to as structure-directing agents (SDAs) since they have been shown to influence the crystalline structure as well as the rate of zeolite formation[3,4]. However, the tailor-made design of a zeolite

Collect. Czech. Chem. Commun. 2008, Vol. 73, Nos. 8–9, pp. 1089–1104

doi:10.1135/cccc20081089

framework for a particular process remains a challenge and there is a continuous effort in both academia and industry devoted to this aim. Bulky organic cations are usually employed in the search for new large-pore materials and many different types of zeolites or zeolite-like materials have been synthesized in this way[5].

As another promising approach, the synthesis of zeolite materials that contain different medium- and large-pore systems of channels (or cavities) in the same structure has been proposed[6]. This could impart additional shape-selectivity effects to the catalyst derived from the particular pore topology, allowing the access of the reactants and the diffusion of the products through one or the other channel system. The synthesis of this type of structures could be favored by the use of a combination of SDAs of different size, i.e., a cooperative structure-directing effect would take place where each SDA would direct the formation of a particular channel or cavity.

In a first instance, we have explored the latter approach using 1-benzyl-1-methylpyrrolidinium (bmp) as the bulky cation in preparations with tetramethylammonium cation (TMA) as the co-SDA. While the use of bmp alone as SDA yielded a complex mixture of crystalline phases, addition of TMA was shown to direct the formation of the ferrierite structure (FER) instead[7]. Ferrierite is a medium-pore type zeolite with a framework formed by two perpendicularly intersecting channel systems of 10- and 8-ring. The structure contains cavities, the ferrierite cage defined by a $[5^8 6^6 8^2]$ polyhedron, which are created by the intersection of the 8-ring channels and the 6-ring channels (parallel to the *c*-axis). A computational study of the samples synthesized in the presence of TMA suggested the location of this SDA in the ferrierite cages while the bmp cation would be located in the 10-ring channels[7].

Following this strategy of synthesis, we have tested the effect that the variation of the co-SDA size exerts on the products of synthesis as well as the effect of the replacement of the bulky 1-benzyl-1-methylpyrrolidinium cation (bmp) by the related but slightly bulkier cation (*S*)-1-benzyl-2-hydroxymethyl-1-methylpyrrolidinium (bmprol) in these preparations. This work presents a comprehensive review of the results obtained so far in the systematic exploration of these variables as well as a preliminary study of the catalytic activity of the ferrierite materials obtained by this approach.

EXPERIMENTAL

Quaternary Ammonium Synthesis

The reagents and the detailed procedure to prepare 1-benzyl-1-methylpyrrolidinium (bmp) hydroxide can be found in ref.[8] The other reagents used were: (*S*)-1-benzylpyrrolidine-2-methanol (Aldrich, 97%), methyl iodide (Fluka, >99 wt.%), ethanol, diethyl ether (stabilized with 6 ppm BHT, Panreac) and ion-exchange resin (Amberlyst IRN78 resin, exchange capacity 4 meq/g, Supelco).

(*S*)-1-Benzyl-2-hydroxymethyl-1-methylpyrrolidinium (bmp) iodide was synthesized by adding 50 g (0.26 mol) of (*S*)-1-benzylpyrrolidine-2-methanol to a solution of 55.66 g of CH_3I (0.39 mol, 50% molar excess) in 200 ml of ethanol. After 5-day stirring at room temperature, ethanol was removed under vacuum at 60 °C. The resulting solid was washed repeatedly with diethyl ether, filtered off and left to dry at room temperature. 70.63 g (0.21 mol, 81% yield) of bmprol iodide was obtained as a yellow solid. Calculated for $C_{13}H_{20}INO$: 46.8% C, 6% H, 4.2% N; found: 47.1% C, 5.9% H, 4.3% N. The iodide salt was converted into the hydroxide by ion exchange with an Amberlyst IRN78 resin. To an aqueous solution of bmprol iodide (70 g, 0.21 mol), 212 g of Amberlyst IRN78 resin was added. After 3-day stirring at room temperature, the resulting solution was filtered and titrated with 0.05 M HCl (Panreac) (using phenolphthalein (Aldrich) as indicator). The amount of bmprol hydroxide obtained as an aqueous solution was 0.17 mol (80% molar yield). This solution was concentrated by partly evaporating the water under vacuum at a temperature lower than 55 °C to prevent the bmprol hydroxide from degradation. By following this procedure a 47 wt.% aqueous solution of bmprolOH was obtained.

Zeolite Synthesis

Zeolite products were obtained from gels with molar composition: 0.06 co-SDA : 0.48 ROH : 0.48 HF : 0.03 Al_2O_3 : 0.94 SiO_2 : 4.30–4.70 H_2O, where ROH designates bmp or bmprol hydroxide and co-SDA designates Na^+, TMA or quinuclidine. The reagents used were: tetraethylorthosilicate (TEOS, Merck, 98 wt.%), aluminium isopropoxide (Fluka, 97 wt.%), tetramethylammonium hydroxide (Aldrich, 25 wt.%, aqueous solution), quinuclidine hydrochloride (Aldrich, 97 wt.%), NaOH (Panreac), 1-benzyl-1-methylpyrrolidinium (bmp) hydroxide (65 wt.% aqueous solution), (*S*)-1-benzyl-2-hydroxymethyl-1-methylpyrrolidinium (bmprol) hydroxide (47 wt.% aqueous solution), and hydrofluoric acid (Panreac, 48 wt.%). The reagents were used without purification. 30.52 g of TEOS and 1.93 g of aluminium isopropoxide were added to a solution containing 35.1 g of bmprol hydroxide and 3.3 g of TMAOH in a polypropylene flask. The solution was left with stirring until ethanol and excess of water were evaporated. Subsequently, 3.06 g of HF were added dropwise. The resulting thick gel (pH ~9.7) was homogenized and transferred into 20-ml Teflon-lined stainless steel autoclaves, which were heated statically at 135 °C under autogenous pressure for selected periods of time. The solid products were recovered by filtration, washed with water and ethanol and dried at room temperature overnight.

Bmprol-TMA-20d was heated in N_2 at 200 °C for 2 h, followed by treatment with a flow of ozone/oxygen (60 ml/min, ca. 2 vol.% O_3) at 200 °C until the organics were completely removed. Ozone in oxygen stream was produced using an ECO-5 ozone generator (Salveco Proyectos, S. L.). Prior to its use in catalysis, the sample was heated in air for 2 h until its temperature reached 550 °C and kept at that temperature for 2 h. Bmp-quin-10d was cal-

cined at 550 °C under continuous flow of N_2 (100 ml/min) for 1 h followed by air (100 ml/min) for 6 h.

Characterization

Solid products were characterized by XRD (Panalytical X'Pro diffractometer using CuKα radiation), C,H,N analysis (Perkin–Elmer 2400 CHN analyzer), TEM (JEOL-2000FX microscope), TGA (Perkin–Elmer TGA7 instrument, heating rate 20 °C/min, air flow 60 ml/min), TG-MS (Perkin–Elmer TGA 7 thermobalance coupled to a Fisons MD-800 quadrupolar mass spectrometer through a transfer line heated at 150 °C; TGA was operated from 30 to 900 °C at 20 °C/min, He flow 100 ml/min) and ^{13}C CP MAS NMR (Bruker AV 400 spectrometer using a BL7 probe). Nitrogen adsorption-desorption isotherms were measured at –196 °C using a Micromeritics Tristar 3000 volumetric apparatus. Specific surface areas were calculated following the BET procedure.

FTIR spectra were recorded in the transmission mode for samples pressed into self-supporting wafers (ca. 6 mg/cm^2 thickness), using a Nicolet 5ZDX FTIR spectrometer provided with an MCT detector. The samples were placed in a glass cell with CaF_2 windows and activated in vacuum at 400 °C for 8 h prior to repeated adsorption treatments with 8 Torr pyridine at 150 °C, followed by degassing at the same temperature for 30 min. The spectra were recorded in the 400–4000 cm^{-1} range, at 4 cm^{-1} resolution, and normalized to a sample thickness of 6 mg/cm^2.

Catalytic Activity Test

The isomerization of *m*-xylene was carried out in a continuous, fixed bed, glass tubular reactor electrically heated, at atmospheric pressure, at 350 °C and a molar ratio of N_2/*m*-xylene = 4. The contact time (W/F) was varied between 0.94–1.34 $g_{cat}/mol_{m\text{-xylene}}$ h. Samples of reaction products were collected at different times on stream, and analyzed by gas chromatography. Initial selectivities for isomerization versus disproportionation of *m*-xylene (I/D ratio) and for *p*-xylene versus *o*-xylene formation (P/O ratio) were obtained from the initial rates of formation of these products. Initial rates were calculated from the initial conversions, X_0, by extrapolating the conversion, X, measured at different times-on-stream, t, using the equation

$$X = X_0 \exp(-kt^{1/2}).$$

In this way differences in the decay rate of the catalytic activity were accounted for.

RESULTS AND DISCUSSION

Synthesis of Zeolites

Table I summarizes the experiments carried out and results obtained with combinations of bulky SDAs and co-SDAs. The organic molecules used in these experiments are shown in Fig. 1.

The results obtained when TMA was used as a co-SDA together with bmp suggested that there is a cooperative structure-directing effect of both cat-

ions in the formation of the ferrierite structure[7]. With this in mind, similar preparations to those of TMA were carried out but using quinuclidine as a co-SDA, instead of TMA. Quinuclidine is a bulkier molecule and its use implies a change in both the size and shape of the molecule used as co-SDA. However, it has been shown to act as SDA for different zeolite preparations usually yielding frameworks with cage-like voids[9] and, in this respect, its performance as SDA is related to that of TMA.

TABLE I
Synthesis of zeolites from gels of composition 0.06 co-SDA : 0.48 ROH : 0.48 HF : 0.03 Al_2O_3 : 0.94 SiO_2 : 4.3–4.7 H_2O, heated at 135°C

Sample	ROH	co-SDA	*t*, days	Product
bmp-quin-10d	bmp	quin	10	FER-related
bmp-quin-30d	bmp	quin	30	FER-related
bmp-Na-10d	bmp	Na^+	10	amorphous
bmp-Na-61d	bmp	Na^+	61	ZSM-12+Beta
bmprol-TMA-20d	bmprol	TMA	20	FER-related
bmprol-TMA-47d	bmprol	TMA	47	FER-related
bmprol-quin-11d	bmprol	quin	11	amorphous
bmprol-quin-30d	bmprol	quin	30	amorphous
bmprol-Na-24d	bmprol	Na^+	24	amorphous+cry[a]
bmprol-Na-52d	bmprol	Na^+	52	unidentified

[a] Cry, cryolite.

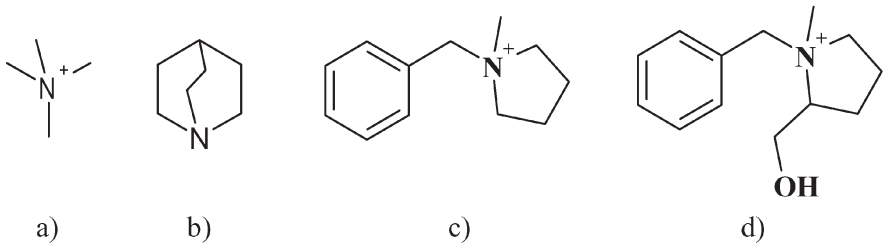

FIG. 1
SDAs and co-SDAs employed in this work: a) tetramethylammonium cation (TMA), b) quinuclidine (quin), c) 1-benzyl-1-methylpyrrolidinium cation (bmp) and d) 1-benzyl-2-hydroxymethyl-1-methylpyrrolidinium cation (bmprol)

The use of quinuclidine led to the crystallization of solids the XRD patterns of which indicate that their structure is related to the family of layered ferrierite materials[10] (Figs 2a and 2b). The structure of this type of materials is built up by the different stacking of ferrierite sheets with the organic molecules used as SDAs located within the layers. Depending on the stacking of the layers, calcination of these solids can result in the formation of a microporous three-dimensional framework by condensation of the silanol groups of adjacent layers[11]. For example, calcination of the PREFER [12] layered precursor gives rise to the formation of the fully connected ferrierite structure while the layer precursor MCM-65 [13] with a different stacking of ferrierite sheets, gives rise to a new framework structure CDO (Fig. 3). In the case of the solids prepared using bmp and quinuclidine, XRD and ^{29}Si MAS NMR suggest that the layered material crystallizing at the first stages progressively condenses during the crystallization process which is thought to be assisted by a reorganization of the organic molecules, from materials richer in bmp to materials richer in quinuclidine, although a fully condensed ferrierite structure is not obtained even at long crystallization times.

Computational studies have shown that, as in the case of TMA, quinuclidine would be preferentially located within the cavities of the ferrierite structure although with lower interaction energy than TMA[10]. Furthermore, these calculations show that quinuclidine would be more stabilized within

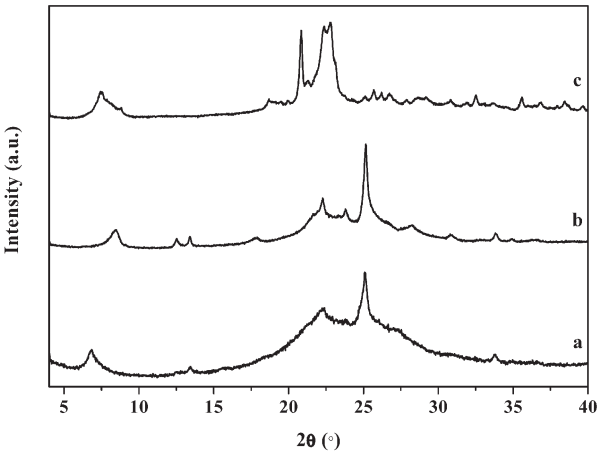

FIG. 2
X-ray diffraction patterns of representative samples synthesized with bmp: bmp-quin-10d (a), bmp-quin-30d (b), bmp-Na-61d (c)

cavities somewhat larger than those actually present in the ferrierite structure. Since the cavities of the ferrierite structure are formed by the condensation of adjacent ferrierite sheets, these results suggest that quinuclidine, being bulkier than TMA, force the sheets away from each other and, therefore, a fully condensed ferrierite structure cannot be obtained with this set of SDAs, as opposed to the preparations with TMA and bmp.

A different situation was found when the nature of the co-SDA was drastically changed by employing a small alkali cation, Na^+, in these preparations. Unlike the former molecules employed as co-SDAs, Na^+ shows a low tendency to direct the formation of zeolites with cage-like voids and, in this sense, it is not considered a cage-forming cation.

When Na^+ was used in these preparations, a mixture of two phases was obtained. TEM allowed the identification of ZSM-12 as one of the components of the mixture. The presence of a very broad diffraction peak at $2\theta \sim 6–8°$ and the reflections at $2\theta \sim 21.4$ and 22.5° in the X-ray diffraction pattern of the mixture (Fig. 2c) suggest that the second phase is probably zeolite beta[14]. ZSM-12 (MTW) possesses a one-dimensional non-interconnected tubular-like channel structure; it belongs among the smallest 12-membered-

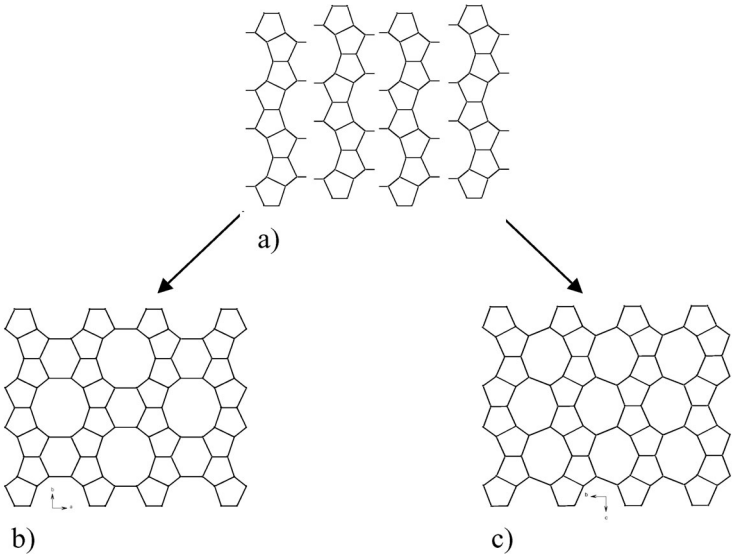

FIG. 3
Stacking of the ferrierite layers (a) can give rise to two structures after calcination, FER (b) or CDO (c)

ring pore zeolites. A projection of the MTW structure with the correct unit cell parameters and symmetry can be obtained by inserting 4-membered rings between ribbons of the ferrierite structure[15], enlarging the pore opening from 10- to 12-membered ring and showing, therefore, that the products obtained in these preparations possess, however, structural features in common (Fig. 4).

EDX analysis performed over crystals of the sample in the TEM microscope showed that they do not contain Na. In addition, the ^{19}F MAS NMR spectrum of this sample (not shown) showed mainly a resonance at –190 ppm, attributed to fluoride in the sodium hexafluoroaluminate cryolite (Na_3AlF_6)[16]. These observations suggest that probably most of the Na^+ added to the gel (and some aluminum as well) is consumed in the formation of this phase and, hence, this cation does not act as a true structure-directing agent but as a composition-directing agent, i.e., its presence alters the gel chemistry, probably reducing the aluminum content in the gel and favoring the crystallization of a silicon-rich zeolite such as ZSM-12.

Nevertheless, it is interesting to note that in these preparations, only the organic co-SDAs direct the products of synthesis towards the formation of ferrierite, a zeolite that possesses channels and cavities in its structure, while in the presence of Na^+, zeolites containing channels but no cavities are obtained. These results also suggest that in these preparations the degree of condensation of the ferrierite layers can be tuned by the proper choice of the organic co-SDA to be hosted in the ferrierite cage.

To further investigate the role of the bulky organic cation in these preparations with co-SDAs, we carried out experiments were the bmp cation was

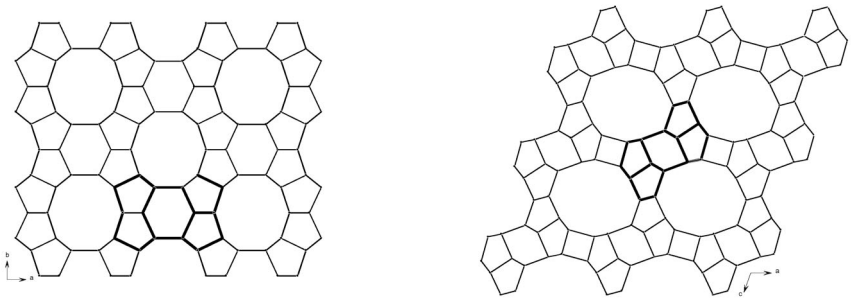

FIG. 4
Projection of a) the FER framework along the pore axis and of b) the MTW framework along the *b* axis, showing the relationship with the two-dimensional projection of FER

replaced by the related chiral cation bmprol in order to examine the effect that small changes in the bulky organic cation exert on the products of syntheses. The main difference between both cations is the presence of a hydroxymethyl group attached to the pyrrolidine ring in the bmprol molecule; therefore, this cation is slightly bulkier than bmp. In addition, the employment of the bmprol cation as structure directing agent is attractive due to the chirality of this molecule, since the CH_2OH group attached to the pyrrolidine ring confers chirality to both, the nitrogen of the pyrrolidine ring and the carbon atom to which this group is attached. The interest in the use of chiral molecules as SDAs relies in the hope that the chirality of the SDA would be transferred to the inorganic framework and would allow the synthesis of a chiral, open framework[17]. Table I summarizes the synthesis conditions employed in these preparations carried out at 135 °C. The corresponding X-ray diffraction patterns of selected products are shown in Fig. 5.

In the preparations with bmprol and TMA as a co-SDA, a ferrierite-related phase was obtained in 20 days. The diffraction pattern of this solid (Fig. 5b) is similar to that of ferrierite although with lower crystallinity than the materials prepared when bmp was used as the bulky cation. Indeed, the total weight loss measured by TGA was around 17%, which is slightly higher than that found for the ferrierite materials synthesized with bmp

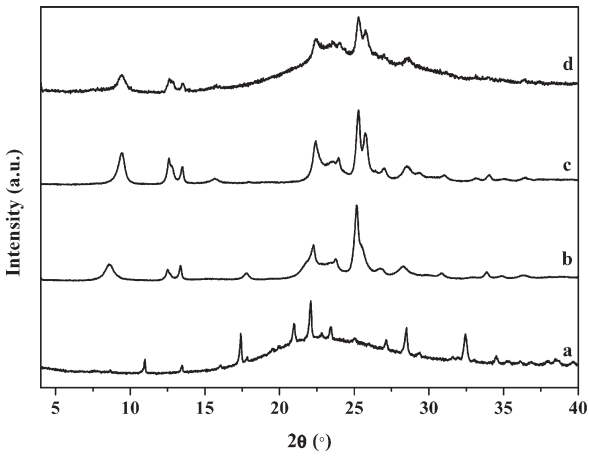

FIG. 5
X-ray diffraction patterns of representative samples, bmprol-Na-52d (a), bmprol-TMA-20d as prepared (b), bmprol-TMA-20d after calcinations (c), bmp-quin-10d calcined (d)

and TMA (usually around 14%). This suggests that the material could have some connectivity defects which would allow to accommodate a higher amount of organic cation. It does not seem that this phase possesses a layered structure similar to that of the samples crystallized with bmp and quinuclidine, since calcination of the material does not shift the lower-angle diffraction peak as much as in the former case. However, we must note that the calcined materials show very similar diffraction patterns in both cases, as it is shown for comparative purposes in Figs 5c and 5d.

Sample bmprol-TMA-20d was further characterized by CHN analysis and ^{13}C CP MAS NMR spectroscopy in order to assess the incorporation of the SDAs within the structure. CHN analysis indicates a C/N ratio of 6.34, i.e., between that of the two organic templates TMA (C/N 4) and bmprol (C/N 13), suggesting that both are occluded within the structure. The ^{13}C CP MAS NMR spectrum of this sample is dominated by a resonance at 59 ppm which can be attributed to the TMA cation (Fig. 6). The resonances that can be attributed to bmprol appear in the spectrum with lower intensity and the signal of the methyl group of this molecule is not clearly distinguished, although the degradation of the molecule through the breaking of such C–N bond is unlikely.

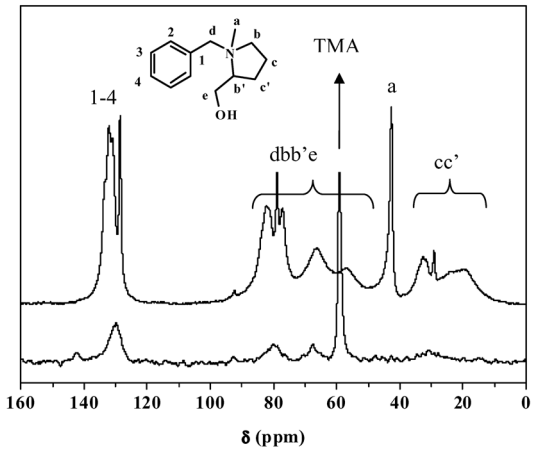

FIG. 6
^{13}C CP MAS NMR spectra of the ferrierite-related sample synthesized with bmprol: bmprol-TMA-20d (bottom) and bmprol iodide salt (top)

To further confirm the incorporation of TMA and bmprol cations into the solid, mass spectrometry combined with thermogravimetric analyses (TG-MS) have been used to study the decomposition processes that take place during the heating of the as-synthesized sample (Fig. 7). The thermogravimetric analysis of this sample in He shows a total weight loss of ~12 wt.%, mainly between 300 and 700 °C. The derivative thermal plot shows two main weight losses, the first one at around 325 °C and the second at around 600 °C. From the mass analyses it can be determined that the first weight loss corresponds to the decomposition of the TMA cation as trimethylamine, as can be seeing monitoring the signal at *m/z* 58. The decomposition of the bmprol cation begins at this temperature and continues up to ~600 °C as can be seen monitoring the signals at *m/z* 84 (corresponding to methylene pyrrolidine), *m/z* 115 (1-methylene pyrrolidine-2-methanol) and *m/z* 91 (benzyl). The peak centered at higher temperature is mainly due to organic fragments, such as propylene with its characteristic signal at *m/z* 39, proba-

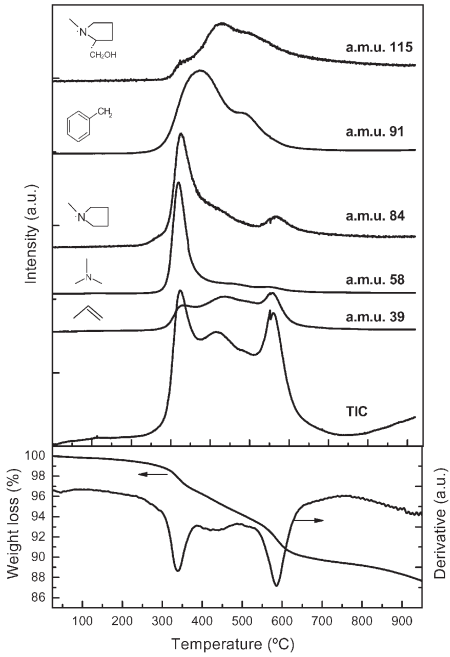

FIG. 7
TG-MS of bmprol-TMA-20d. Bottom: thermogravimetric and derivative plots. Top: total ion current (TIC) and MS signal intensities for selected *m/z* values indicating the different products obtained

bly due to the cracking of the remaining SDA molecules which have not been decomposed previously and which can be occluded in sterically hindered positions of the framework. Therefore, the results obtained by these techniques indicate that both organic cations remain intact within the as-synthesized material.

Furthermore, the chemical shift corresponding to TMA in the ^{13}C CP MAS NMR spectrum is close to that obtained for the ferrierite synthesized with bmp and TMA (57.8 ppm) and appears in the typical range of TMA cations trapped in zeolitic cages[18]. This suggests a similar location of the organic molecules within the microporous framework as that proposed for the ferrierite solids synthesized with bmp and TMA. Since the 10-MR channels of the ferrierite structure can be formed by assembling ferrierite cages around the bulkier SDA used in each case, it is tempting to propose that the bulkier nature of bmprol could be the reason for the differences found in the crystallinity between these two samples.

In the preparations where bmprol was used together with quinuclidine as a co-SDA, only amorphous materials were obtained at crystallization times as long as 30 days. Therefore, in this case, the combination of two bulky organocations has a critical effect on the formation of ferrierite or ferrierite-related phases as compared with the bmp preparations that yielded this kind of products at shorter crystallization times.

In the preparations using bmprol and Na^+ as a co-SDA, amorphous material and some cryolite were obtained at short crystallization times, while at longer times of synthesis, a yet unidentified phase was obtained, the XRD pattern of which is shown in Fig. 5a. Again, the formation of ferrierite or ferrierite-related materials is not observed when Na^+ is used as co-SDA, as already found for the preparation containing bmp as the bulky cation.

Acidity and Catalytic Test

FTIR spectroscopy has been used to characterize the acid sites present in sample bmprol-TMA-20d after calcination. For comparison, a ferrierite sample (FER-1) was prepared in alkaline (NaOH) medium[19]. The sample was calcined using the same procedure as described previously for bmprol-TMA-20d. However, after this treatment, FER-1 was ion-exchanged repeatedly with an ammonium chloride solution and calcined in air at 550 °C.

Figure 8 shows the spectra of both samples after outgassing at 400 °C. The spectra show bands at 3600 and 3745 cm^{-1}, assigned to bridging hydroxyl groups (Si–OH–Al) in ferrierite[20] and terminal silanols, respectively. An additional band at ca. 3650 cm^{-1} can be observed in the spectrum of FER-1

and, with weak intensity, in bmprol-TMA-20d, which can be tentatively assigned to OH species associated to extra-framework aluminum or defect sites. When pyridine was adsorbed on the samples at 150 °C, the formation of pyridinium ions took place, giving rise to the characteristic band at 1545 cm^{-1} (not shown). Concomitantly, the intensity of the band at 3600 cm^{-1} decreased, showing the loss of bridging OH groups due to proton transfer from these Bronsted acid sites. When the samples remained in contact with pyridine at 150 °C for several minutes, a substantial decrease of the 3600 cm^{-1} band intensity was observed, although the band was not completely removed, indicating that a part of the Brønsted sites were not accessible to pyridine. Therefore, prolonged exposure to pyridine was used in order to allow its diffusion through all the accessible zeolite pores. After pyridine adsorption for up to 4 h, the band at 3600 cm^{-1} was still present in the spectrum of bmprol-TMA-20d (Fig. 8b), revealing that 40% of the bridging hydroxyls are located in sites that cannot be reached by pyridine. These results are in line with those previously reported for ferrierite[20]. In contrast, the band at 3600 cm^{-1} was nearly completely removed for the reference sample FER-1, evidencing full accessibility of pyridine to these acid sites. Interestingly, pyridine adsorption did not decrease the intensity of the band at 3650 cm^{-1}, showing that this sample also possesses hydroxyl groups that are not accessible to pyridine.

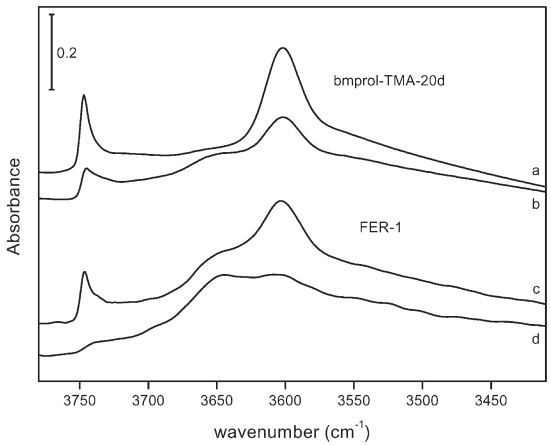

FIG. 8
FTIR spectra in the O–H stretching vibrations region of bmprol-TMA-20d and FER-1 after outgassing at 400 °C (a, c) and subsequent adsorption of pyridine at 150 °C for 4 h (b, d)

Catalytic test reactions are very useful for determining the structure and dimensions of intracrystalline void space of zeolites and molecular sieves. The catalytic activity of some of the materials synthesized in this work was tested in the isomerization of *m*-xylene (Table II). The selectivity to the different isomerization and disproportionation products (indicated by the I/D ratio) furnished valuable information on the distribution of acid centers in the crystals. According to the results collected in Table II, the para/ortho selectivity (P/O ratio) of the catalyst synthesized following a conventional synthesis route in the presence of sodium ions (FER-1) corresponds to that expected for medium-pore zeolites[21], quite similar to that previously reported for ferrierite catalysts[22]. Practically no disproportionation products are detected. This is also in agreement with the crystal size of this sample, 3 × 2.5 μm. Indeed, the activity of this sample is nearly three times higher than that of the sample synthesized with bmprol. This result is in agreement with the fact that only a fraction of nearly 40% of the total acid sites present in the framework are capable of interacting with pyridine in the latter sample, as discussed above. Moreover, the P/O ratio is remarkably low, quite close to that of large-pore zeolite catalysts, and even some trimethylbenzenes resulting from disproportionation are detected. This behavior is

TABLE II
Activity and selectivity of selected catalysts in the isomerization of *m*-xylene

Catalyst	*m*-xylene conversion, %	Initial reaction rate, 10^{-2} mol/g h	P/O Ratio	I/D Ratio
bmp-quin-10d	8.9	5.7	1.4	7.5
bmprol-TMA-20d	2.2	1.4	1.5	13.0
FER-1[a]	3.7	3.9	4.6	46.2

[a] Reference sample synthesized according to ref.[19]

TABLE III
Textural properties of selected ferrierite and ferrierite-related catalysts

Catalysts	BET area, m^2/g	Micropore area, m^2/g	External area, m^2/g
bmp-quin-10d	445	308	137
bmprol-TMA-20d	261	198	63

in agreement with the high external surface area of the sample (Table III), and suggests that a large fraction of the accessible acid sites are located on the external surface of the catalysts where they contribute remarkably to the total activity. High surface area in this case is not unexpected, because the as-synthesized material does not seem to possess a fully condensed three-dimensional structure. Furthermore, the layered ferrierite material synthesized from bmp and quinuclidine results, after calcinations, in a catalyst characterized by a high external surface area (Table III), much higher than that of the sample synthesized from bmprol and TMA. The activity and selectivity pattern of this sample again reveals the contribution of the external surface to the reaction, as evidenced by a low P/O ratio and a relatively low I/D ratio. Moreover, the reaction rate of this catalyst is higher than that of FER-1, probably also due to the contribution of the external surface.

CONCLUSIONS

The preparations containing bmp as the bulky cation and an organic molecule as co-SDA have been shown to produce ferrierite and ferrierite-related materials, depending on the size of the organocation used as co-SDA. In contrast, a mixture of zeolites ZSM-12 and Beta is obtained in the presence of Na^+, a cation with lower tendency to direct the formation of particular cages. This cation does not remain within the zeolites and only the bulky bmp acts as SDA, directing the synthesis towards a product with a single type of channel system. The replacement of bmp by a related although slightly bulkier cation, bmprol, produced a ferrierite-related phase only in the experiments where TMA was used as co-SDA. The results indicate that both the bulky and the smaller co-SDA influence the products of these preparations and small changes in one or the other affect the products of synthesis. A close relationship between the acid and textural properties and the catalytic behavior of these materials has been observed.

We are thankful for the financial support of the Spanish Ministry of Education and Science (MEC), project CTQ2006-06282. R. García acknowledges the J. A. E. contract (CSIC). A. B. Pinar acknowledges MEC for a FPU grant.

REFERENCES

1. Breck D. W.: *Zeolite Molecular Sieves*. Wiley, New York 1974.
2. Weitkamp J.: *Solid State Ionics* **2001**, *131*, 175.
3. Gies H., Marler B.: *Zeolites* **1992**, *12*, 42.
4. Cundy C. S., Cox P. A.: *Chem. Rev*. **2003**, *103*, 663.

5. http://www.iza-structure.org/databases/
6. Corma A., Rey F., Valencia S., Jordá J. L., Rius J.: *Nat. Mater.* **2003**, *2*, 493.
7. Pinar A. B., Gómez-Hortigüela L., Pérez-Pariente J.: *Chem. Mater.* **2007**, *19*, 5617.
8. Pinar A. B., García R., Pérez-Pariente J.: *Collect. Czech. Chem. Commun.* **2007**, *72*, 666.
9. Grünewald-Lüke A., Marler B., Hochgräfe M., Gies H.: *J. Mater. Chem.* **1999**, *9*, 2529.
10. García R., Gómez-Hortigüela L., Díaz I., Sastre E., Pérez-Pariente J.: *Chem. Mater.* **2008**, *20*, 1099.
11. Knight L. M., Miller M. A., Koster S. C., Gatter M. G., Benin A. I., Willis R. R., Lewis G. J., Broach R. W.: *Stud. Surf. Catal. Sci.* **2007**, *170*, 338.
12. Schereyeck L., Caullet P., Mougenel J. C., Guth J. L, Marler B.: *Microporous Mater.* **1996**, *6*, 259.
13. Dorset D. L., Kennedy G. J.: *Phys. Chem. B* **2004**, *108*, 15216.
14. García R., Díaz I., Pérez-Pariente J.: *Microporous Mesoporous Mater.* (Accepted).
15. LaPierre R. B., Rohrman A. C., Schlenker J. L., Jr., Wood J. D., Rubin M. K., Rohrbaugh W. J.: *Zeolites* **1985**, *5*, 346.
16. Scholz G., Korup O.: *Solid State Sci.* **2006**, *8*, 678.
17. Davies M. E.: *Top. Catal.* **2003**, *25*, 3.
18. a) Fan W., Shirato S., Gao F., Ogura M., Okubo T.: *Microporous Mesoporous Mater.* **2006**, *89*, 227; b) Hayashi S., Suzuki K., Hayamizu K.: *J. Chem. Soc., Faraday Trans. 1* **1989**, *85*, 2973.
19. Plank C. J., Rosinski E. J., Rubin M. K.: U.S. 4016245 (1977); *Chem. Abstr.* **1977**, *86*, 178180x.
20. Wichterlová B., Tvarůžková Z., Sobalík Z., Sarv P.: *Microporous Mesoporous Mater.* **1998**, *24*, 223.
21. Martens J. A., Pérez-Pariente J., Sastre E., Corma A., Jacobs P. A.: *Appl. Catal.***1988**, *45*, 85.
22. Rachwalik R., Olejniczak Z., Sulikowski B.: *Catal. Today* **2006**, *114*, 211